FEASIBILITY STUDY OF MAGNETITE EXTRACTED FROM INDONESIAN MILL SCALE THROUGH DIRECT REDUCTION PROMOTED BY GRAPHITE BASED CARBON

Deni Shidqi Khaerudini[1,2], Windi Yulistia[3], Idha Royani[3], Dita Rahma Insiyanda[1], Sagir Alva[2], Ramlan[3]

[1] *Research Center for Physics, Indonesian Institute of Sciences (LIPI) Gd.440-442 Kawasan Puspiptek Serpong, Tangerang Selatan Banten 15314 Indonesia E-mail: deni.shidqi@mercubuana.ac.id; deni.shidqi.khaerudini@lipi.go.id*

[2] *Department of Mechanical Engineering, Mercu Buana University, South Meruya No. 1 Jakarta 11650 Indonesia*

[3] *Department of Physics, Faculty of Mathematics and Natural Sciences, University of Sriwijaya, Indralaya Ogan Ilir, Palembang, Sumatera Selatan 30662 Indonesia*

Received 19 February 2019
Accepted 31 July 2019

ABSTRACT

Mill scale (MS) is a solid by-product of hot or cold rolling processes in steelmaking industry. It contains iron oxide in the form of magnetite, hematite and wustite. It has fairly high iron content, which is predominantly in the form of hematite (that of metallic Fe amounts only to 0.2 wt. %). The present investigation refers to the development of a direct reduction of MS aiming to increase the magnetite phase presence. Graphite based carbon (GBC) is used as a reducing agent. The procedure includes raw materials (MS, GBC) pre-heating for 30 min at 300°C. The subsequent step refers to a reduction of MS/GBC mixtures (of vol. % content of 20:80, 30:70, 50:50, 70:30, 80:20) in the course of high energy milling within 30 min. Pellets are then obtained at a loading of 100 MPa for 1 min and sintering for 1 h at 1300°C in an inert atmosphere. They are crushed into a powder, which is separated from the impurities present by a magnetic separator. The reduction product is characterized using an X-ray diffractometer (XRD), a vibrating sample magnetometer (VSM) and Gauss meter.

Keywords: industrial waste, mill scale, magnetite, graphite based carbon, direct reduction.

INTRODUCTION

Magnetite (Fe_3O_4) draws a considerable attention because of its attractive properties providing applications in magnetic storage media, solar energy transformation, electronics and magnetoelectronics, biomedicine, catalysis, waste water treatment [1 - 9]. The crystallites size and shape as well as the domain structure (phase) defining their physico-chemical properties factor determine these applications [10]. Fe_3O_4 nano- or microscale powders are produced [11 - 13] by an ultrasonic chemical co-precipitation and a solvothermal route application, which are found promising because of their simplicity and productivity. But the raw materials required refer to high purity commercial materials (such as ferrous chloride or ferrous nitrate).

The low cost and the large scale production are essential for magnetite industrial application. An alternative in this respect can be found in the use of waste-based raw materials. Mill scale (MS) is a waste material from the steelmaking industry. It is considered rich in iron (mainly magnetite, hematite, wustite). The high iron oxide content of the mill scale provides its potential use as a raw material of magnetite (Fe_3O_4) production. Such an approach will provide a decreased cost and utilization of the industrial waste obtained. The objective of the investigation presented is to develop a novel direct reduction method of obtaining magnetite from MS us-

ing graphite based carbon (GBC) as a reducing agent.

EXPERIMENTAL

The industrial MS of PT Krakatau Steel, Cilegon, Indonesia was chosen as a raw material. Its chemical composition referred to 74.24 wt. % of total Fe (including 0.20 wt. % of metal Fe and 52.02 wt. % of Fe_2O_3), 0.25 wt. % of SiO, 0.97 wt.% of CaO, and MgO to 100 %. The graphite material was sieved (150 mesh) and preheated for 30 min at 300°C. It was added to MS aiming to obtain mixtures of MS/GBC vol. % ratios of 20:80, 30:70, 50:50, 70:30 and 80:20. They were pressed for 1 min at 100 MPa to form pellets and sintered within 1 h at 1300°C in an inert atmosphere. After the subsequent cooling, the pellets were crushed in a mortar into a powder and the corresponding impurities were separated by a magnetic separator. The product was additionally crushed within 30 min using a ball mill with a milling speed of 300 RPM. The ball to powder ratio was equal to 5:1 wt. %. Then the powder was pressed statically at 300 MPa for 1 min and sintered at 550°C for 1 h in air.

The purity and the lattice structure of MS/GBC powder and pellets were examined by XRD (Rigaku SmartLab) using Cu-Kα (λ = 1.541862 Å) radiation source over the angular range of $20^o \leq 2\theta \leq 70^o$. The scanning was collected at a step width of 0.01°. Rietveld refinement was performed by using High Score Plus™ [14]. The saturation magnetization and the surface magnetic field of the powder were measured by using a vibrating sample magnetometer (VSM-250 Electromagnetic). The pellets were analyzed by Gauss meter (Impulse Magnetizer X-Series, Magnet-Physik).

RESULTS AND DISCUSSION

MS/GBC powders of vol. % ratios of 30:70, 50:50 and 70:30 are subjected to XRD analysis at a room temperature. The patterns obtained are shown in Fig. 1. The results show that magnetite (Fe_3O_4) without any impurity is found in all samples. The difference observed refers only to the peak shape, mainly at (113), (004), and (044) reflection indices. The latter indicate the difference in the lattice parameters obtained. The XRD results verify

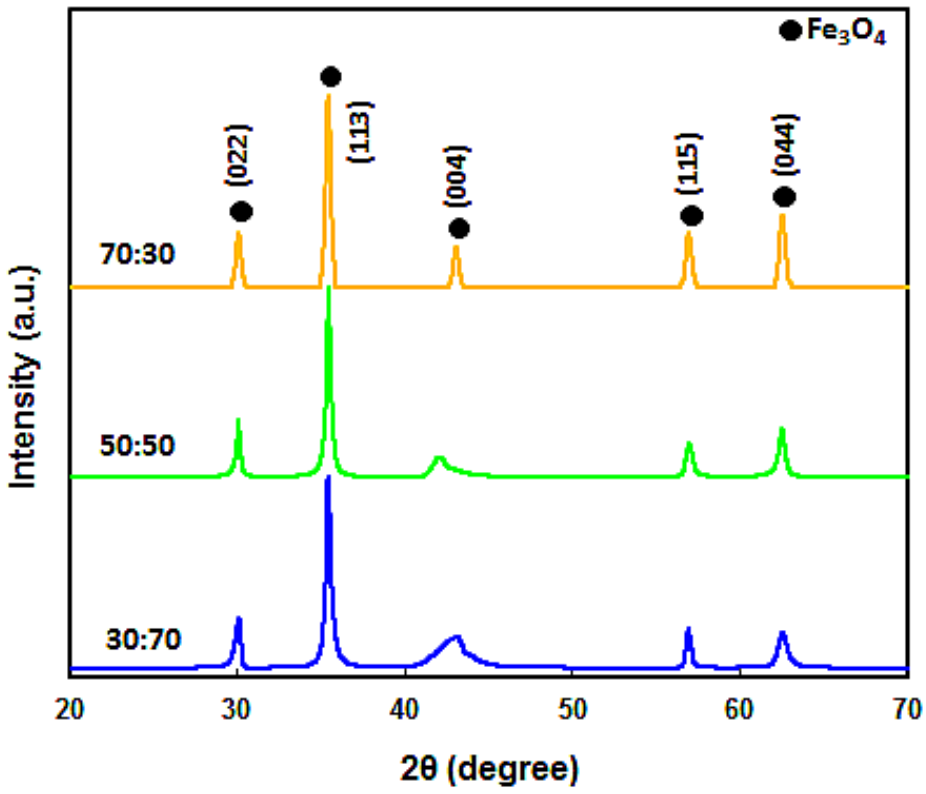

Fig. 1. XRD profiles of MS/GBC powders containing vol. % ratios of 30:70, 50:50, and 70:30 vol. % after calcination for 1 h at 1300°C in an inert atmosphere.

Table 1. Space group and lattice constants of MS/GBC powder calcined at 1300°C.

MS:GBC (vol.%)	Space group	a (Å)	Crystallite size (Å)	ρ_{cal} (g/cm^3)	R_p (%)	R_{exp} (%)	R_{wp} (%)	χ^2	Ref. Code
30:70	F*d*-3*m*	8.40554	203.43	5.1785	7.7575	9.4416	9.7137	1.05846	98-007-5627
50:50	F*d*-3*m*	8.40681	218.45	5.1761	7.7781	9.5249	9.7546	1.04881	98-004-3001
70:30	F*d*-3*m*	8.40806	238.80	5.1738	7.8792	9.5273	9.8911	1.07784	98-008-2234

that the direct reduction applied is suitable to reduce the mill scale powder (originally containing various iron oxide phases) to magnetite. The sequence followed can be described by:

Gasification

$$C(s) + CO_2(g) \rightarrow 2CO(g) \quad (1)$$

Reduction

$$3Fe_2O_3(s) + CO(s) \rightarrow 2Fe_3O_4(s) + 3CO_2(g) \quad (2)$$

The following explanation is provided on the ground of the XRD data obtained and Eqs. (1) and (2) : (i) the indirect reduction of carbon to carbon monoxide (endothermic) takes place following the Bouduard reaction [15]; (ii) the reduction of hematite (Fe_2O_3) to magnetite (Fe_3O_4) proceeds as shown by the XRD results (Fig. 1). The Bouduard reaction is endothermic and which is why it requires high (appropriate) temperature (1300°C in this case). It is essential to provide the heat required within the bulk of MS/GBC mixture.

The crystal structure information is obtained by refinement analysis application. The R factor values referring to the Rietveld refinement of MS/GBC powder can be determined by using High Score Plus software. For instance, the resulted refinements referring to MS:GBC=30:70 vol. % are as follows: R_p = 7.7575, R_{exp} = 9.4416, R_{wp} = 9.7137, and χ^2 = 1.05846). The chi square (χ^2) stands for $(R_{wp}/R_{exp})^2$ factor indicating the fit between the experimental data and the model [16]. The refined lattice parameters including the values of the R factors and χ^2 of all MS/GBC powders (30:70, 50:50, and 70:30 vol. %) are listed in Table 1. The pattern of MS/GBC composite powders refers to Fd-3m space group. The calculated lattice parameter of MS:GBC = 30:70 vol.% amounts to 8.40554 Å, while the calculated density is equal to 5.1785 g cm^{-3}. The results obtained show that GBC content increase results in smaller lattice parameters or a finer crystallite size. This can be explained with the finer crystallite size of GBC [17].

The hysteresis loops of all MS/GBC powder variations and the single loop of MS:GBC=20:80 vol. % shown in Fig. 2(a) and 2(b), respectively, are indicative of a low remanence magnetization values. The magnifying remanence-coercivity magnifying loops are shown in Fig. 2(c). They are indicative of the ferrimagnetic nature of MS/GBC powder, which in turn determines the expression of 'soft' ferromagnetic (small coercive force) properties. The data referring to the magnetic properties parameters (Fig. 2(d)) and the remanence-coercivity of all MS/GBC powders studied is listed in Table 2.

Table 2. Magnetic properties of MS/GBC composite powder.

MS:GBC (vol. %)	Saturation (G)	Remanence (G)	Coercivity (Oe)
20:80	8127.35	1725.16	482.70
30:70	4800.67	1098.47	521.31
50:50	4577.06	988.67	476.83
70:30	3158.06	672.44	466.59
80:20	2986.30	621.53	458.29

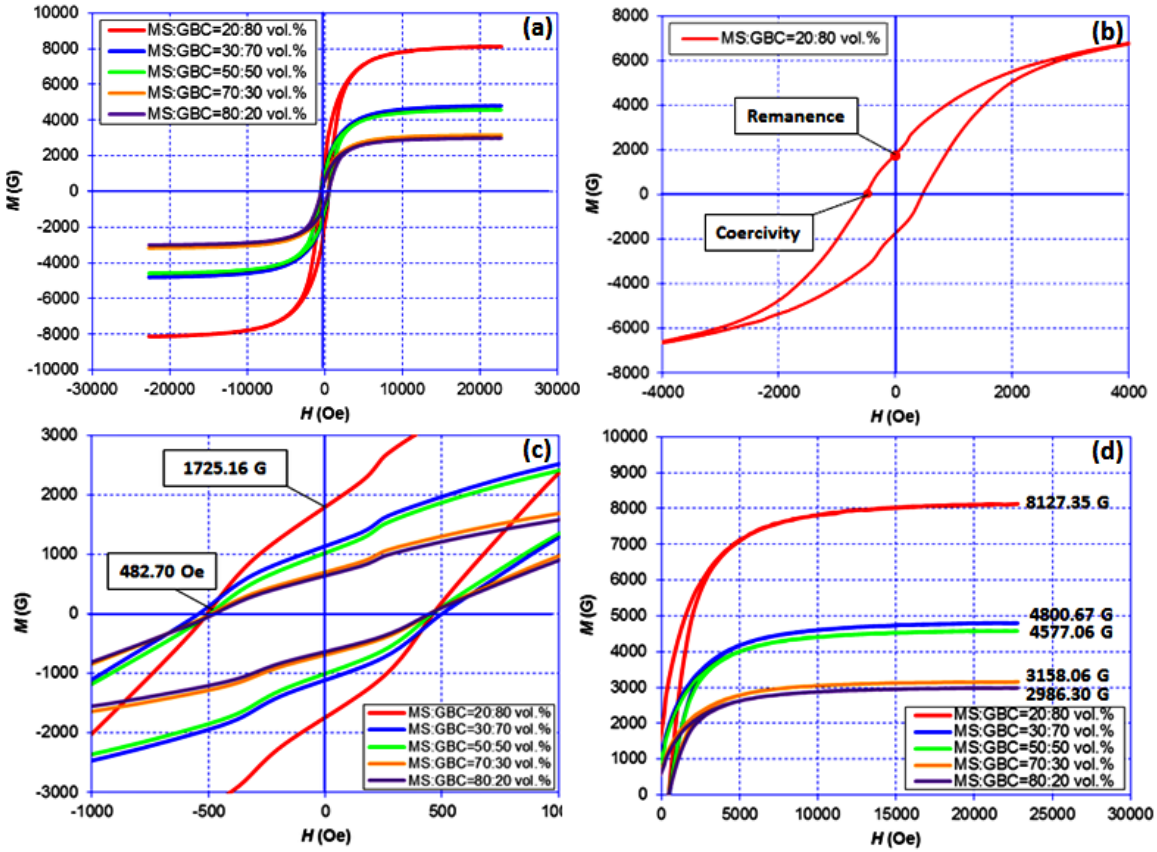

Fig. 2. Magnetic properties of MS/GBC composite powders: (a) hysteresis loops; (b) a hysteresis loop of MS:GBC=20:80 vol. %; (c) remanence-coercivity and (d) all variations saturation.

In general, the saturation-remanence values decrease with GBC content decrease. This can be explained with GBC contribution to MS reduction as shown by the XRD analysis (Fig. 1 and Table 1). It is evident that the saturation-remanence values decrease with crystallite size increase (or theoretical density decrease) of all samples. The coercivity values which are also affected by GBC content (compositions crystallite size) are included in Table 2. They decrease from around 482.70 Oe for the MS:GBC = 20:80 vol. % to a minimum value of around 458.29 Oe for MS:GBC = 80:20 vol. %. The highest coercivity value (a larger coercive force) of around 521.31 Oe is observed in case of MS:GBC = 30:70 vol. %. This is probably due to structural changes, specifically at (004) peak as previously illustrated by the XRD results (Fig. 1). The magnetic 'softness' of the structure obtained is due to the opposite sign of the magnetorestriction constant of the crystallite and the residual amorphous matrix, which provide the reduction and the average magnetorestriction compensation [18]. The low values of coercivity correspond to an easy movement of the domain walls as the magnetic field changes its magnitude and direction. The relative area within the hysteresis loops must be thin and narrow. This 'soft' magnetic behavior can be used in devices subjected to alternate magnetic fields requiring low energy losses.

The powder is compacted through sintering in air at 550°C. This 'treatment' is carried out to examine the effect of the surface/external magnetic field by applying the Gauss method in view of the oxidation condition treatment. The XRD patterns of the sintered samples of certain compositions (30:70, 50:50 and 70:30 vol. %) are comparable to those of the corresponding powders. They are shown in Fig. 3. All sintered samples indicate phase and structural changes which refer to a transit from a single phase of magnetite (Fe_3O_4) to a mixed phase containing predominantly hematite (Fe_2O_3). Fig. 3(b) illustrates the XRD peaks phase evolution in case of a sintered and powdered MS:GBC = 30:70 vol. % sample. The magnetite phase remaining after the refinement of

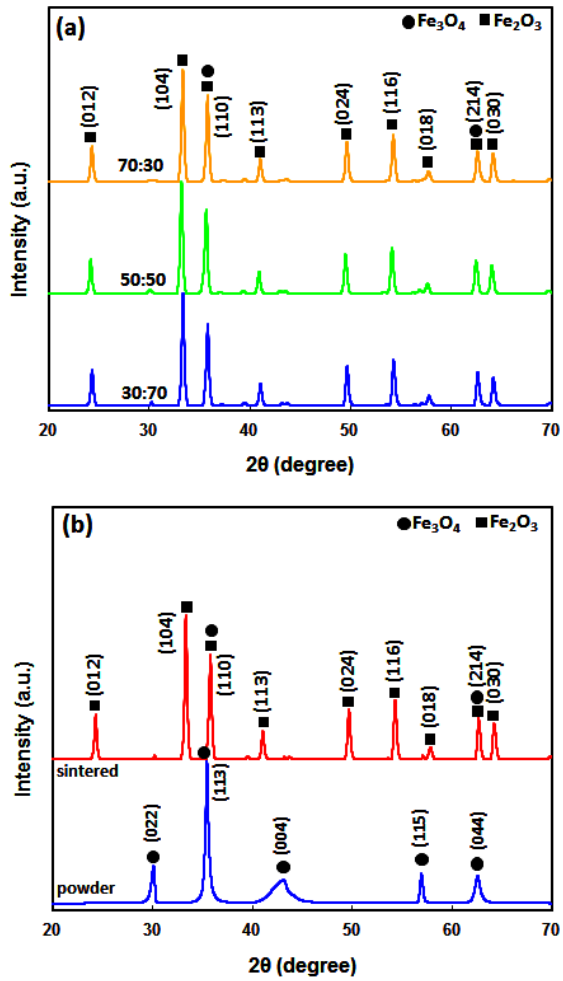

Fig. 3. Refined X-ray diffractions of (a) a sintered MS:GBC= 30:70 vol. % (1h, 550°C, an air atmosphere); (b) sintered and powdered MS:GB = 30:70 vol. %.

certain compositions (30:70, 50:50 and 70:30 vol. %) amounts to 3.4 %, 8.0 %, and 9.4 %, respectively. These results indicate that GBC is initially assessed and then oxidized to CO_2 (g). The most probable reason is presented as follows: the contact particle interface (a local reaction) of MS-GBC sintered sample provides a faster progressive reduction process when compared to the process in the mixture powder. This leads to decrease of the magnetite phase with GBC content increase. There is another possible explanation. The magnetite (Fe_3O_4) is sometimes formulated as ($FeO.Fe_2O_3$) containing both Fe^{2+} and Fe^{3+} (an unbalanced state). The reaction of Fe_3O_4 with O_2 (from the air) at a certain temperature leads to Fe_2O_3. This is in correspondence with the general iron oxide transformation pathway involving the magnetite progressive oxidation to maghemite, which is finally

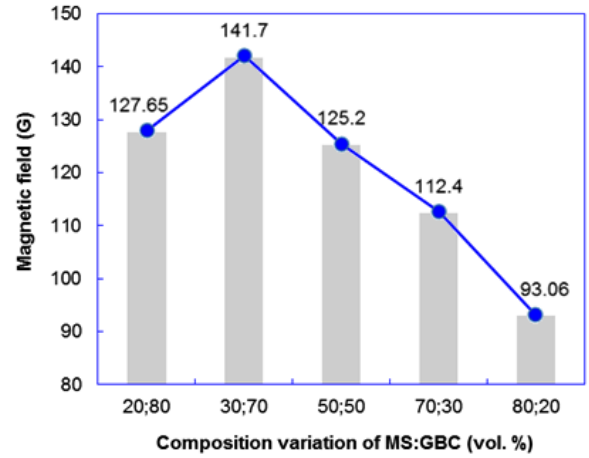

Fig. 4. Sintered samples surface magnetic fields.

transformed to hematite [19]. That is why the sintered sample of MS:GBC = 30:70 vol.% has the lowest magnetite presence (3.4 %).

The resulting external magnetic field examined by Gauss meter is shown in Fig. 4. It appears that the structural changes of the sintered samples degrade dramatically the magnetic behavior of the corresponding materials. The results show clearly that MS:GBC = 30:70 vol.% sample has the highest (stable) magnetic field compared with those of the other compositions, which may look unexpected. However, in view of the phase transformation pathway considered previously, several iron oxides may be simultaneously present during the sintering. This implies that the co-existence of hematite and magnetite can complicate the magnetic structure and in turn can worsen the observed surface magnetic behavior [20]. Hence, the magnetite phase present is not the only parameter controlling the external (surface) magnetic behavior of the sample.

CONCLUSIONS

In summary, MS is successfully reduced by GBC in the course of a solid state reduction followed by calcination within 1 h at 1300°C in an inert atmosphere. The XRD analysis carried out shows that the powders contain pure magnetite of Fd-3m cubic lattice. The crystallite size decreases with GBC content increase. The hysteresis loops observed show low coercivity indicative of samples 'soft' magnetic properties. The mixture containing MS to GBC vol. % ratio of 30:70 shows the best magnetic behavior both in a powdered and a sin-

tered state. These findings suggest that a good balance between the crystallite size and the phase stability can be achieved in obtaining magnetite from MS. This is of importance in respect to potential industrial applications and steelmaking waste treatment.

Acknowledgements

The authors are grateful to the Research Center for Physics- LIPI for the facilities and the technical support provided. They acknowledge the partial financial support offered by Pusat Penelitian UMB through Skim Dosen Prima (Project #000539). D.S.K. highly appreciates the fruitful discussions with A.P. Tetuko.

REFERENCES

1. P. Tartaj, M.P. Morales, S.V. Verdaguer, T.G. Carreno, C.J. Serna, The preparation of magnetic nanoparticles for applications in biomedicine, J. Phys. D: Appl. Phys., 36, 2003, R182-R197.
2. S. Wu, S. Aizhi, Z. Fuqiang, J. Wang, X. Wenhuan, Z. Qian, A.A. Volinsky, Fe_3O_4 magnetic nanoparticles synthesis from tailings by ultrasonic chemical coprecipitation, J. Mater. Lett., 65, 2011, 1882-1884.
3. T.L.Phan, N.T.Dang, T.A.Ho, J.S. Rhyee, W.H.Shon, K.Tarigan, T.V.Manh, Magnetic and magnetocaloric properties of $Sm_{1-x}Ca_xMnO_3$ (x = 0.88) nanoparticles, J. Magn. Magn .Mater., 443, 2017, 233-238.
4. S. Bedanta, Supermagnetism in magnetic nanoparticle, Dissertation, Universitat Duisburg-Essens, Germany, 2006.
5. A. Yan, X. Liu, G. Qiu, H. Wu, R. Yi, N. Zhang, J. Xu, Solvothermal synthesis and characterization of size-controlled Fe_3O_4 nanoparticles, J. Alloy. Compd., 458, 1-2, 2008, 487-491.
6. S. Nie, E. Starodub, M. Monti, Insight into magnetite's redox catalysis from observing surface morphology during oxidation, J. Am. Chem. Soc., 135, 27, 2013, 10091-10098.
7. T. Yamada, K. Morita, K. Kume, H. Yoshikawa, K. Awaga, The solid-state electrochemical reduction process of magnetite in Li batteries: in situ magnetic measurements toward electrochemical magnets, J. Mater. Chem. C, 2, 2014, 5183-5188.
8. U. Meisen, H. Kathrein, Influence of particle size, shape and particle size distribution on properties of magnetites for the production of toners, J. Imaging Sci. Technol., 44, 6, 2000, 508-513.
9. C.T. Yavuz, J.T. Mayo, W.W. Yu, Low-field magnetic separation of monodisperse Fe_3O_4 nanocrystals, Science, 314, 5801, 2006, 964-967.
10. J. Lee, S.G. Kwon, J.G. Park, T. Hyeon, Size dependence of metal–insulator transition in stoichiometric Fe_3O_4 nanocrystals, Nano Lett., 15, 7, 2015, 4337-4342.
11. H.E. Ghandoor, H.M. Zidan, M.M.H. Khalil, M.I.M. Ismail, Synthesis and some physical properties of magnetite (Fe_3O_4) nanoparticles, Int. J. Electrochem. Sci., 7, 2012, 5734-5745.
12. S.M. Bello, R.A.M. Luckie, L.F. Santos, J.P. Hinestroza, V.S. Mendieta, Size-controlled synthesis of Fe_2O_3 and Fe_3O_4 nanoparticles onto zeolite by means of a modified activated-coprecipitation method: effect of the HCl concentration during the activation, J. Nanopart. Res., 14, 11, 2012, 1242.
13. W.Q Jiang, H.C. Yang, S.Y. Yang, H.E. Horng, J.C. Hung, Y.C. Chen, C.Y. Hong, Preparation and properties of superparamagnetic nanoparticles with narrow size distribution and biocompatible, J. Magn. Magn. Mater., 283, 2004, 210-214.
14. T. Degen, M. Sadki, E. Bron, U. König, N. Gwilherm, The HighScore suite, Powder Diffraction 29, S2, 2014, S13-S18.
15. A.L. Yergey, F.W. Lampe, Carbon gasification in the Boudouard reaction, Fuel, 53, 4, 1974, 280-281.
16. B.H. Toby, R factors in Rietveld analysis: How good is good enough?, Powder Diffraction, 21, 1, 2006, 67-70.
17. D.S. Khaerudini, G.B. Prakoso, D.R. Insiyanda, H. Widodo, F. Destyorini, N. Indayaningsih, Effect of graphite addition into mill scale waste as a potential bipolar plates material of proton exchange membrane fuel cells, IOP Conf. Series: Journal of Physics: Conf. Series, 985, 2018, 012050.
18. J.S. Val, J. González, in: A. Méndez-Vilas, J. Díaz (Eds.), Microscopy: Science, Technology, Applications and Education, Microscopy Book Series, Formatex Research Center, Badajoz, Spain, 2010, 3, 4 p. 1620.
19. P.F. Barbosa, L. Lagoeiro, R. Scholz, L.M. Graça, N. Mohallem, Magnetite-hematite transformation: correlation between natural and synthetic features, Miner Petrol, 109 3, 2015, 329-337.
20. M. Ahmadzadeh, C. Romero, J. McCloy, Magnetic analysis of commercial hematite, magnetite, and their mixtures, AIP Advances, 8, 2018, 056807-1 - 056807-6.